Data-Driven Dynamic Equivalents for Power System Areas From Boundary Measurements

Andrija T. Sarić, Mark T. Transtrum, and Aleksandar M. Stanković

***Abstract*—The paper describes an algorithm for parameter identification of a dynamic equivalent for an external subsystem, based solely on the available online measurements in boundary buses and branches. Static equivalent part is represented by equivalent impedances from boundary buses (ones that separate the internal and external subsystems) and calculated using the modified (minimum loss) radial, equivalent, and independent method. Parameter identification of synchronous generator (SG)-based equivalent (for predominantly production external areas), dynamic load (DL)-based equivalent (for predominantly load external areas), or (SG + DL)-based equivalent (for mixed external areas) in fictitious buses is performed by Levenberg–Marquardt weighted least-square nonlinear optimization, which minimizes the variances between available online measurements and transient responses of the reduced power system. The IEEE 14-bus and 441-bus real-world test systems are used to illustrate and test the proposed power system equivalent derivation technique.**

***Index Terms*—Dynamic equivalent, online measurement, parameter identification, REI equivalent, WLS nonlinear optimization.**

I. Introduction

DYNAMIC models of power systems (for example, electromechanical models used in transient analysis) have reached size of thousands of dynamic elements (SGs, automatic voltage regulators, turbines, distributed energy resources etc.) and tens of thousands of buses. However, their fidelity has not kept up. Specifically, models have been unable to quantitatively match recordings of major events (for example [1]).

There exists agreement in industry that for large-scale power systems, it is neither practical nor necessary to always perform dynamical studies (such as the electromagnetic transient analysis, online dynamic security assessment, or design of controls) with full detailed dynamic models. Analysts are typically interested in the behavior of a certain part of the system. This part is called *internal* or *study subsystem* and the rest of the power system is referred to as *external subsystem* [2]. More specifically, for model simplification purposes the power system is divided into three parts: 1) *detailed model* (non-reduced and measured part represented as a white box model), 2) *connection (transmission) network* (measured and non-reduced part), and 3) *dynamic equivalent* (non-measured and reduction-based part represented as a gray box model).

The reduction of the computational effort has historically been a key motivation for equivalents (static and dynamic). Today, it is dwarfed in importance by the need to manage uncertainty in large interconnections. Several trends contribute to model fidelity issues:

1) inadequate data exchanges among entities in a large interconnection, some of which compete directly in the energy market;
2) lack of information about the actual operating point across the interconnections covered by multiple local state estimators;
3) the actual list of components connected in a large interconnection at a given time is not known to any single entity;
4) a larger model is not necessarily better when it comes to tuning to match recorded transients (many well-instrumented blackouts like the 2003 Eastern Interconnection blackout in North America confirm);
5) there exist challenges in maintaining dynamic models up-to-date even within an entity, and it is unreasonable to expect it for a whole interconnection.

We are interested in maintaining the ability to physically interpret estimated parameters, so we consider typical models for source and load buses. In a large interconnection which is only partially known to each participant, it is important to have physical intuition as a tool to detect gross errors in parameter estimates and model structure. This interpretability also helps in the case of multiple uses within the same organization. Model reduction can also be a multi-stage process, and it is to our advantage to keep it traceable by limiting types of allowed objects.

The question of practical identifiability of model parameters from measurements is of universal importance, and frames the problem considered here. The establishment of entities that compete in the energy market necessarily reduces incentives to collaborate on technical issues and to exchange data. Thus, future electric energy providers will increasingly rely on

Manuscript received December 19, 2017; revised April 24, 2018 and June 28, 2018; accepted August 12, 2018. Date of publication August 29, 2018; date of current version December 19, 2018. This work was supported in part by ARPA_E under contract DE-AR0000223, in part by the CURENT Engineering Research Center of the National Science Foundation and the Department of Energy under NSF Award Number EEC-1041877, and in part by the Ministry of Education and Science of the Republic of Serbia, under project III-42004. Paper no. TPWRS-01889-2017. *(Corresponding author: Aleksandar M. Stanković.)*

A. T. Sarić is with the Department for Power, Electronic and Communication Engineering of the Faculty of Technical Sciences, University of Novi Sad, Novi Sad 21000, Serbia (e-mail: asaric@uns.ac.rs).

M. K. Transtrum is with the Department of Physics and Astronomy, Brigham Young University, Provo, UT 84602 USA (e-mail: mktranstrum@byu.edu).

A. M. Stanković is with the Department of Electrical Engineering and Computer Science, Tufts University, Medford, MA 02155 USA (e-mail: astankov@ece.tufts.edu).

Color versions of one or more of the figures in this paper are available online at http://ieeexplore.ieee.org.

Digital Object Identifier 10.1109/TPWRS.2018.2867791

dynamical models, and on communication and computer technology to maintain a stable system operation. Such models will have to be validated mostly from (locally) available prior information and from available online measurements [3].

Classical methods for computing static network equivalents are Ward and REI equivalents (from numerous references on the subject, see [4]–[7]). The Ward equivalent is a multi-port Thevenin construct, possibly with added reactive power support. The information from external subsystem is required for derivation. In general, REI equivalent is a lossless network representation of a set of base case injections (*"zero power balance network")*.

Complementing and extending static equivalents, dynamic equivalents have a key role in large-scale power system analysis. The typical target for dynamic equivalents is to define equivalent SGs, so that the reduced network transient stability features are as close as possible to the original power system. There exist hundreds of references on this topic, including methods based on coherency, synchrony, modal analysis, artificial intelligence etc. (for an overview, see [8], [9]).

Attempts to use online data to improve dynamical models of key components, e.g., SGs, have a long history in power systems. First successes in employing general dynamical systems concepts like trajectory sensitivity go back more than a quarter century [10], [11]. That particular approach has been extended to hybrid systems in [12]. Another influential approach that is based on local information extracted from the measurement Jacobian is described in [13]. To deal with ill-conditioning of the parameter estimation problem, this reference proposes that a subset of parameters of the SG model be fixed to prior values, while estimating the remaining parameters from the available data (denoted as the subset selection method). In the sequel, we only list references of immediate relevance to our development here. For example, [14] considers parameter estimation for a single SG and re-casts SG's parameter identification in a differential-algebraic equations (DAEs) framework. References [15], [16] show that some parameters of the dynamic model are unidentifiable when using only the steady-state data (online measurements) before disturbance, but identifiable when using dynamic data during disturbance. References [17], [18] consider the same overall setup involving Phasor Measurement Unit (PMU)-derived measurements.

In this paper, we propose a two-stage procedure for identification of static and dynamic parts of external equivalent, respectively described as:

1) Determination of static equivalent impedances from boundary buses (in retained area) to fictitious buses (in reduced area), in a modified REI procedure [2], [19], that tunes the parameters to achieve fixed voltages closer to typical operating conditions.
2) Identification of the dynamic parameters of SG-based equivalent (SGe) for dynamic generation, dynamic load based equivalent (DLe) for predominantly load areas and composite (SGe+DLe) based equivalent for mixed areas from available boundary measurements, using a WLS-based procedure (instead of combining *known* parameter sets of different dynamic components).[1]

The two stages represent two portions of a hybrid procedure, combining the prior static information about the interconnection (modified REI) with a data-driven algorithm to estimate the model parameters.

The proposed method does not require data about the external system, which is the initial assumption in almost all algorithms for dynamic equivalents (Ward- or REI-based). While it may well be that a hybrid solution will prove most advantageous in practice, in this paper we wanted to quantify capabilities of the measurement data-driven approach.

The basic idea for the proposed algorithm and preliminary results are shown in [20]. This algorithm is improved in several important aspects:

i) introduced DLe for predominantly load external equivalents;
ii) explored (SGe+DLe) for mixed external equivalents;
iii) information geometry is applied for selection of sloppy (unidentifiable) parameters in dynamic models;
iv) use of Levenberg-Marquardt algorithm for ill-conditioned optimization problems [21];
v) robustness of the method for different operation scenarios is improved by the proposed three-step approach (optimization, re-optimization and robustness testing);
vi) the algorithm is tested for more complex test cases and on a real-world test system.

The outline of the paper is as follows. Section II describes the power system model used for parameter identification; Section III provides the algorithm for parameter identification of external dynamic equivalents; in Section IV we present numerical studies for IEEE 14-bus and 441-bus real-world test systems, while Section V contains our recommendations and conclusions. SGe and DLe dynamic models are described in Appendices.

II. Dynamic Model for Parameter Identification

The power system under study is divided into three parts: 1) measured part ('Detailed model'), 2) observed transmission network, and 3) non-measured part of power system (to be replaced with 'Dynamic equivalent'):

1) SGs (with appropriate controls: turbine, automatic voltage regulator, power system stabilizers and others) and other production units (for example, for wind and solar) in 'Detailed model' part are modeled by physics-based mathematical equations.
2) Transmission network is modeled by actual topology and branch models (lines, transformers and others) in the non-reduced part of power system.

[1]Assumed dynamic model of equivalent areas depends on their production and load structures. Without loss of generality, our methodology is described with SGe and DLe dynamic models, as these tend to be adequate choices for typical power system structures today.

3) Dynamic equivalent is modeled by static equivalent branches and dynamic models represented by SGe and/or DLe.

Dynamic models of power system components are typically written in DAEs form:

$$\dot{\boldsymbol{x}} = \boldsymbol{f}(\boldsymbol{x}, \boldsymbol{z}, \boldsymbol{p}, t) \tag{1}$$

$$\boldsymbol{0} = \boldsymbol{g}(\boldsymbol{x}, \boldsymbol{z}, \boldsymbol{p}, t) \tag{2}$$

where $\boldsymbol{x}$ is the vector of (differential) state variables, $\boldsymbol{z}$ are the algebraic variables, $\boldsymbol{p}$ are parameters and t is the time variable. System measurement vector is assumed to be of the form:

$$\boldsymbol{y} = \boldsymbol{h}(\boldsymbol{x}, \boldsymbol{z}, \boldsymbol{p}, t) \tag{3}$$

The parameter vector ($\boldsymbol{p}$) is into be estimated from available online measurements ($\boldsymbol{y}$), and there typically exists some prior information about parameters, often in the form of plausible ranges for each. The least-square optimization formulation of the identification problem is by far the most prevalent in the literature.

It turns out that the key quantities in the case of least-square identification are parametric sensitivities whose dynamics are described by the following equations [14], [22]:

$$\frac{d}{dt}\left(\frac{\partial \boldsymbol{x}}{\partial \boldsymbol{p}}\right) = \frac{\partial \boldsymbol{f}(\boldsymbol{x}, \boldsymbol{z}, \boldsymbol{p}, t)}{\partial \boldsymbol{x}} \cdot \frac{\partial \boldsymbol{x}}{\partial \boldsymbol{p}} + \frac{\partial \boldsymbol{f}(\boldsymbol{x}, \boldsymbol{z}, \boldsymbol{p}, t)}{\partial \boldsymbol{z}} \cdot \frac{\partial \boldsymbol{z}}{\partial \boldsymbol{p}} + \frac{\partial \boldsymbol{f}(\boldsymbol{x}, \boldsymbol{z}, \boldsymbol{p}, t)}{\partial \boldsymbol{p}} \tag{4}$$

$$\boldsymbol{0} = \frac{\partial \boldsymbol{g}(\boldsymbol{x}, \boldsymbol{z}, \boldsymbol{p}, t)}{\partial \boldsymbol{x}} \cdot \frac{\partial \boldsymbol{x}}{\partial \boldsymbol{p}} + \frac{\partial \boldsymbol{g}(\boldsymbol{x}, \boldsymbol{z}, \boldsymbol{p}, t)}{\partial \boldsymbol{z}} \cdot \frac{\partial \boldsymbol{z}}{\partial \boldsymbol{p}} + \frac{\partial \boldsymbol{g}(\boldsymbol{x}, \boldsymbol{z}, \boldsymbol{p}, t)}{\partial \boldsymbol{p}} \tag{5}$$

$$\frac{\partial \boldsymbol{h}}{\partial \boldsymbol{p}} = \frac{\partial \boldsymbol{h}(\boldsymbol{x}, \boldsymbol{z}, \boldsymbol{p}, t)}{\partial \boldsymbol{x}} \cdot \frac{\partial \boldsymbol{x}}{\partial \boldsymbol{p}} + \frac{\partial \boldsymbol{h}(\boldsymbol{x}, \boldsymbol{z}, \boldsymbol{p}, t)}{\partial \boldsymbol{z}} \cdot \frac{\partial \boldsymbol{z}}{\partial \boldsymbol{p}} + \frac{\partial \boldsymbol{h}(\boldsymbol{x}, \boldsymbol{z}, \boldsymbol{p}, t)}{\partial \boldsymbol{p}} \tag{6}$$

These equations are linear in terms of sensitivities, but the matrices involved do vary along a system trajectory.

III. Parameter Identification of External Dynamic Equivalent

The dynamic equivalent is composed from REI branches [2], [19], SGe and DLe, where recommended dynamic models for SGe are outlined in [11], [12] and for DLe (Static Voltage- Dependent (SVD) + Induction Machine (IM)-based equivalents) in [23]. Dynamic models used for SGe and DLe are summarized in Appendices A and B, respectively.

Parameter identification of dynamic equivalent is performed from available online measurements, where it is assumed that all border points ($i \in \aleph$, where $\aleph$ is m-dimensional set of border buses between retained and external subsystems) are equipped with complete set of electrical measurements (V_i, θ_i, P_{bi} and Q_{bi}, where $\underline{V}_i = V_i e^{j\theta_i}$ is measured complex voltage in ith border bus [obtained from measured voltage magnitude (V_i) and angle (θ_i)] and $\underline{S}_{bi} = P_{bi} + jQ_{bi} = \sum_{j \in \Re_i} \underline{S}_{bij}$ is complex power flow from ith bus [obtained from measured active (P_{bi}) and reactive power flows (Q_{bi})] to external subsystems, respectively, where $\Re_i$ is the total number of buses in the external subsystems connected with ith border bus–see Fig. 1.

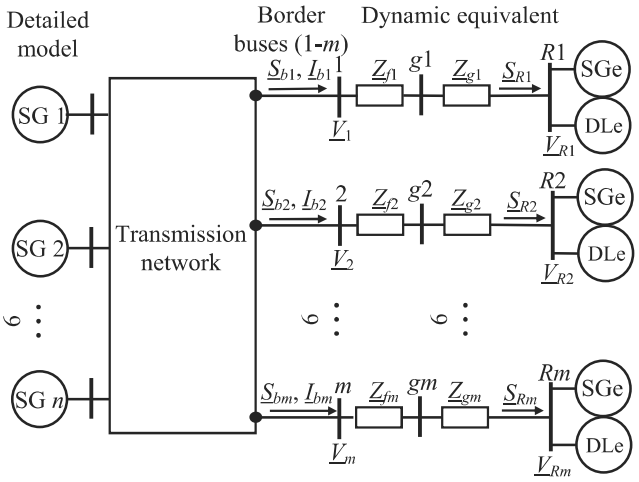

Fig. 1. REI-based equivalent branches.

The proposed algorithm has the following steps:

Step 1: Calculation of external equivalent impedances (inner $\underline{Z}_{fi}; i \in \aleph$, and outer $\underline{Z}_g$), based on the static REI minimum loss equivalent approach, detailed described in our reference [20].

Step 2: Calculation of equivalent measurements on SGe, DLe or (SGe+DLe) level from available online boundary measurements ($\underline{V}_i$, $i \in \aleph$ and $\underline{S}_{bi} = \sum_{j \in \Re_i} \underline{S}_{bij}$), as (see Fig. 1):

$$\underline{S}_{Ri} = P_{Ri} + jQ_{Ri} = \underline{S}_{bi} - (\underline{Z}_{fi} + \underline{Z}_{gi})|\underline{I}_{bi}|^2 \tag{7}$$

$$\underline{V}_{Ri} = \underline{V}_i - (\underline{Z}_{fi} + \underline{Z}_{gi})\underline{I}_{bi} \tag{8}$$

where:

$$\underline{Z}_{gi} = R_{gi} + jX_{gi}$$

$\underline{I}_{bi} = \underline{S}^*_{bi}/\underline{V}^*_i$ is complex current flow from ith bus toward the external subsystems (calculated from available online measured values V_i, θ_i, P_{bi} and Q_{bi}).

Step 3: Selection of quantities at the end of the REI-based equivalent branches (for transient analysis of reduced power system):

- PV bus (for SGe and (SGe+DLe)):

$$P_{gi} = -P_{Ri}; V_{Ri} = |\underline{V}_{Ri}| \tag{9}$$

- PQ bus (only DLe):

$$P_{li} = P_{Ri}; Q_{li} = Q_{Ri} \tag{10}$$

Step 4: Classification of the parameters for SGe dynamic model is based on the sloppiness analysis [22, Section VI]. Initial (uncertain) parameters are (see Appendix A for details): H, x_d, x_q, x'_d and x'_q, while

the remaining parameters (D, T'_{d0} and T'_{q0}) are fixed, resulting in a well-behaved estimation task (see detailed eigenvalue analysis of the measurement Hessian matrix in [22, Section VI]). In our simulations, we neglect the automatic voltage regulator and turbine dynamic in equivalent branches (see Section IV for details).

Classification of the parameters for DLe dynamic model is also based on the sloppiness analysis [23, Section V.B]. Initial (uncertain) parameters are (see Appendix B for details): x_s and r_r (for IMe part) and p_p (for SVDe part, where assumed that $p_p = q_p, p_z = q_z$, $p_z = 1 - p_p - p_i$ and $q_z = 1 - q_p - q_i$), while the remaining parameters (r_s, x_r, x_μ, p_i and q_i) are fixed.

Step 5: Calculation of first partial derivatives of system measurement vector with respect to uncertain parameters $\boldsymbol{J_p}(t) = \boldsymbol{J}_{\boldsymbol{p},t} = \partial \boldsymbol{h}(t)/\partial \boldsymbol{p}; t = 1, 2, \ldots, T$ (the Jacobian matrix for parameter vector $\boldsymbol{p}$).

Step 6: WLS-based fitting of a dynamic equivalent model (SGe-, DLe- or (SGe+DLe)-based) to experimental data by minimization of the sum of weighted squares of the components of the N-dimensional (N is total number of elements in measurement vector $\boldsymbol{h}$, where index ℓ denotes a component; T is number of discrete time steps with a time step denoted as t) error (residual) vector $\boldsymbol{r}_t(\boldsymbol{p}) = \boldsymbol{h}_t - \boldsymbol{h}_t(\boldsymbol{p})$ as:

$$\hat{\boldsymbol{p}} = \min \left\{ \frac{1}{2} \left\| \sum_{t=1}^{T} \boldsymbol{W} \boldsymbol{r}_t(\boldsymbol{p}) \right\|^2 \right\}$$

$$= \min \left\{ \frac{1}{2} \sum_{\ell=1}^{N} w_\ell \sum_{t=1}^{T} r_{\ell.t}^2(\boldsymbol{p}) \right\} \tag{11a}$$

subject to constraints:[2]

$$\boldsymbol{p}^{\min} \le \boldsymbol{p} \le \boldsymbol{p}^{\max} \tag{11b}$$

where $\boldsymbol{W}$ is diagonal weighting matrix, with values of particular elements discussed in Section IV.

Introducing cumulative vectors for analyzed time interval (T):

$$\boldsymbol{r}(\boldsymbol{p}) = \begin{bmatrix} \boldsymbol{r}_1(\boldsymbol{p}) \\ \boldsymbol{r}_2(\boldsymbol{p}) \\ \vdots \\ \boldsymbol{r}_T(\boldsymbol{p}) \end{bmatrix} = \boldsymbol{h} - \boldsymbol{h}(\boldsymbol{p}); \boldsymbol{h} = \begin{bmatrix} \boldsymbol{h}_1 \\ \boldsymbol{h}_2 \\ \vdots \\ \boldsymbol{h}_T \end{bmatrix};$$

$$\boldsymbol{h}(\boldsymbol{p}) = \begin{bmatrix} \boldsymbol{h}_1(\boldsymbol{p}) \\ \boldsymbol{h}_2(\boldsymbol{p}) \\ \vdots \\ \boldsymbol{h}_T(\boldsymbol{p}) \end{bmatrix}; \boldsymbol{J_p} = \begin{bmatrix} \boldsymbol{J}_{\boldsymbol{p}1} \\ \boldsymbol{J}_{\boldsymbol{p}2} \\ \vdots \\ \boldsymbol{J}_{\boldsymbol{p}T} \end{bmatrix}$$

[2]This constraint represents limited parameter values and additional constraints for estimated parameters (for example, $x_d \ge x_q > x'_q \ge x'_d \ge 0$ and other [24, eqs. (4.43)–(4.45)]).

the necessary condition for optimum in (11a) is:

$$\boldsymbol{0} = -\frac{\partial \boldsymbol{h}(\boldsymbol{p})}{\partial \boldsymbol{p}} \boldsymbol{W} [\boldsymbol{h} - \boldsymbol{h}(\boldsymbol{p})]$$

$$= -\boldsymbol{J}_{\boldsymbol{p}}^T \boldsymbol{W} [\boldsymbol{h} - \boldsymbol{h}(\boldsymbol{p}) - \boldsymbol{J_p} \Delta \boldsymbol{p}] \tag{12}$$

which provides the system of linear equations for uncertain parameter increments:

$$[\boldsymbol{J}_{\boldsymbol{p}}^T \boldsymbol{W} \boldsymbol{J_p}] \Delta \boldsymbol{p} = \boldsymbol{J}_{\boldsymbol{p}}^T \boldsymbol{W} [\boldsymbol{h} - \boldsymbol{h}(\boldsymbol{p})] \tag{13a}$$

Reference [25] applies the Levenberg-Marquardt algorithm for similar measurement-based derivation of a dynamic equivalent. However, the matrix $\boldsymbol{J}_{\boldsymbol{p}}^T \boldsymbol{W} \boldsymbol{J_p}$ is often ill-conditioned, with eigenvalues spanning several orders of magnitude. Therefore, unless the initial guess is very good, the Gauss-Newton method will typically take a large (and unknown) number of iterations, and may fail to converge altogether. To remedy these shortcomings, it was suggested in [21] to regularize the Levenberg-Marquardt method by increasing "damping" of $\boldsymbol{J}_{\boldsymbol{p}}^T \boldsymbol{W} \boldsymbol{J_p}$ matrix with a diagonal cutoff as:

$$[\boldsymbol{J}_{\boldsymbol{p}}^T \boldsymbol{W} \boldsymbol{J_p} + \lambda \boldsymbol{D}^T \boldsymbol{D}] \Delta \boldsymbol{p} = \boldsymbol{J}_{\boldsymbol{p}}^T \boldsymbol{W} [\boldsymbol{h} - \boldsymbol{h}(\boldsymbol{p})] \tag{13b}$$

where $\boldsymbol{D}^T \boldsymbol{D}$ is a positive-definite diagonal matrix representing the relative scaling of the parameters (vector $\boldsymbol{p}$) and λ is a damping parameter adjusted by the algorithm (in our simulations $\lambda = 10$).

Step 7: Check the convergence criterion (ε is a convergence threshold):

$$\max \{\Delta \boldsymbol{p}\} \le \varepsilon \tag{14}$$

If the convergence criterion (14) is not satisfied replace parameter vector estimate as $\boldsymbol{p} = \boldsymbol{p} + \Delta \boldsymbol{p}$ and continue iterative process with *Step 5*; otherwise the final parameter estimate is $\hat{\boldsymbol{p}} = \boldsymbol{p}$.

The parameter identification is divided into three steps:

Step A: Initially optimized parameters.

Step B: Improved re-optimized parameters.

Step C: Verification of parameters (robustness testing).

The equilibrium point at the time of study (for example, before disturbance for transient analysis) is represented by available online boundary measurements (time instant just before disturbance) and by specified steady-state quantities in PQ and PV buses in retained part of the power system. These values are used as input data for the calculation of the extended power flow solution (determining the pre-disturbance condition and algebraic variables).

IV. Application

Our simulations are based on PSAT for transient analysis simulations, which is a suite of freely available Matlab routines (well documented in [26]) to which we have added our code for the parameter estimation algorithm described in Section III.

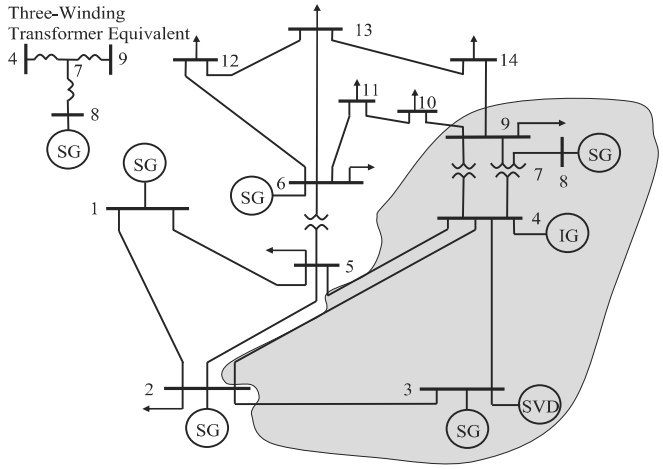

Fig. 2. Single-line diagram of IEEE 14-bus test system with analyzed test.

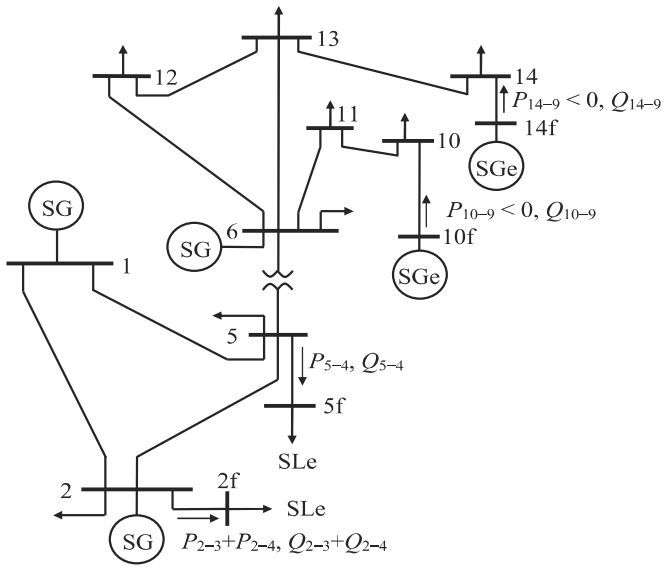

Fig. 3. Reduced IEEE 14-bus test system (Step A: Initially optimized parameters).

Numerical tests are performed for modified IEEE 14-bus [26, Fig. 2.4, also see Appendix D in this reference for detailed input data] and real-world 441-bus test systems.

A. IEEE 14-Bus Test System

The modified IEEE 14-bus test system (added dynamic loads: SVD-based in bus 3 and IG-based in bus 4) is composed from (see Appendix A for details of SG modelling and Appendix B for DL modelling):

- 53 state variables:
  - 24 for SGs (two 6-order and three 4-order models);
  - 20 for automatic voltage regulators (five 4-order models);
  - 6 for turbines (two 3-order models), and
  - 3 for IG (one 3-order model).
- 55 algebraic variables:
  - 14×2 bus voltage magnitudes (V) and angles (θ);
  - 5×4 for SGs (P_m, v_f, v_d and v_q);
  - 5×1 for automatic voltage regulators (v_{fe});
  - 2×1 for turbines (v_{ft}), and
  - 2×1 for IM (v_d and v_q).

The test system is subjected to the three-phase short circuit in Bus 1 (see Fig. 2) at $t, = 1.0$ s, which cleared after 150 ms.

For this test example buses 2, 5, 10 and 14 are border buses between the retained and the external subsystem, in accordance with Fig. 2. These buses are equipped with complete set of electrical measurements (bus voltage magnitude/angle and power flows to external subsystem). Based on these measurements, the parameters of the external equivalent impedances between bus X (2, 5, 10, and 14) and bus X_f are calculated in *Step 1*, with details in [20]. Buses 3, 4, 7, 8, and 9 are part of the dynamic equivalent, and are to be eliminated. 18 online measurements are available: V_2, V_5, V_{10}, V_{14}, θ_2, θ_5, θ_{10}, θ_{14}, P_{2-3}, P_{2-4}, P_{5-4}, P_{10-9}, P_{14-9}, Q_{2-3}, Q_{2-4}, Q_{5-4}, Q_{10-9}, and Q_{14-9} (see Figs. 2 and 3).

Equivalent branches obtained in *Step 1* (impedances and other quantities for equivalent buses, $i \in \aleph$) are in Table I.

Step A: Initially optimized parameters.

Initial parameter optimization is based on the direction of active power flows from internal to external subsystem. Based on the results presented in Table I, the dynamic equivalent scenario with two SGes and two Static Load equivalents (SLes) were investigated − see Fig. 3. We thus conclude that the active power flows in branches $10-10$f and $14-14$f are from the external (equivalent) to the original (retained) part of the power system. This means that SG dynamic models (with uncertain parameters) are connected at buses 10f and 14f. For identification, from the described online measurements and calculated equivalent impedances, a new set of equivalent measurements is: 1) $V_{10f}(t)$, $\theta_{10f}(t)$, $P_{g10f}(t)$, and $Q_{g10f}(t)$ (for SGe in bus 10f), and 2) $V_{14f}(t)$, $\theta_{14f}(t)$, $P_{g14f}(t)$, and $Q_{g14f}(t)$ (for SGe in bus 14f).

Please note that the equivalent part is small and has strongly coupled lines, making loop-flows possible; thus, it is addressed in a single optimization.

Previous studies have established that full 6-order SGe's parameter identification is difficult from typical online measurements [5], [9], [12], [13], [16]. In this paper, the SGes in the external subsystem are assumed to be described by a 4-order dynamic model (see Appendix A for details) without automatic voltage regulator and turbine dynamic models. Note that these assumptions yield conservative results, and can be relaxed as needed (turbine dynamics are slow and often have a small influence in transient analysis; additional fine tuning for typical automatic voltage regulator may be needed).

Given the conclusions of [22], the constant and initial values (suggested in *Step 4*) of electrical/mechanical parameters for estimation (in corresponding units) respectively are:

- $T'_{d0} = 4.60$, $T'_{q0} = 0.54$; $D = 2$.
- $2H = 11.75$, $x_d = 1.25$, $x'_d = 0.232$, $x_q = 1.22$, $x'_q = 0.715$.

The estimated SGe's parameters obtained by the proposed nonlinear WLS-based estimation (Section III) are shown in

TABLE I
CALCULATION OF EQUIVALENT BRANCHES (IEEE 14-BUS TEST SYSTEM)

Bus i	$\underline{V}_i$ [p.u.]	$\Re_i$	$\underline{S}_{bi}$ [p.u.]	$\underline{Z}_{fi}+\underline{Z}_{gi}$ [p.u.]	$\underline{V}_{Ri}$ [p.u.]	$\underline{S}_{Ri}$ [p.u.]
2	1.042–j0.082	2–3, 2–4	1.165+j0.068	0.0017+j0.0007	1.040–j0.083	1.163+j0.068
5	1.011–j0.130	5–4	0.532–j0.049	–0.0652–j0.0173	1.045–j0.122	0.550–j0.045
10	1.000–j0.197	10–9	–0.093+j0.013	–0.0111+j0.0032	1.001–j0.196	–0.093+j0.013
14	0.977–j0.222	14–9	–0.139–j0.001	0.0268+j0.0131	0.981–j0.221	–0.140–j0.001

TABLE II
OPTIMAL PARAMETER IDENTIFICATION FOR SGES (IEEE 14-BUS TEST SYSTEM)

	Bus 10f					Bus 14f				
	Mechanical parameter	Electrical parameters				Mechanical parameter	Electrical parameters			
	$2H$ [MWs/MVA]	x_d [p.u.]	x'_d [p.u.]	x_q [p.u.]	x'_q [p.u.]	$2H$ [MWs/MVA]	x_d [p.u.]	x'_d [p.u.]	x_q [p.u.]	x'_q [p.u.]
Initial	11.750	1.250	0.232	1.220	0.715	11.750	1.250	0.232	1.220	0.715
Optimized	3.210	1.196	0.118	1.097	0.477	4.810	1.172	0.108	1.322	0.404

TABLE III
SENSITIVITY ANALYSIS OF RESIDUALS AND OPTIMIZATION CRITERION TO WEIGHTING FACTORS IN WLS-BASED OPTIMIZATION (IEEE 14-BUS TEST SYSTEM)

	$\sum_{t=1}^{T} r_{V_i}^2$	$\sum_{t=1}^{T} r_{\theta_i}^2$	$\sum_{t=1}^{T} r_{P_{g,i}}^2$	$\sum_{t=1}^{T} r_{Q_{g,i}}^2$	$\sum_{\ell=1}^{N} w_\ell \sum_{t=1}^{T} r_{\ell,t}^2$
$w_{V,P_g}=100000\,;\, w_{\theta,Q_g}=1$	0.3536 + 0.2776 = 0.6312	24.5658 + 24.5648 = 49.1306	0.9567 + 0.4422 = 1.3989	0.6183 + 0.4609 = 1.0792	203052.784
$w_{V,\theta,P_g}=100000\,;\, w_{Q_g}=1$	0.1636 + 0.1798 = 0.3434	24.7294 + 24.7617 = 49.4911	0.5830 + 0.3847 = 0.9677	0.4941 + 0.3910 = 0.8851	5080225.783
$w_{V,\theta,P_g,Q_g}=100000$	0.3536 + 0.2776 = 0.6312	24.5229 + 24.5158 = 49.0387	0.9567 + 0.4422 = 1.3989	0.6183 + 0.4609 = 1.0792	5223979.135
$w_{V,P_g,Q_g}=100000\,;\, w_{\theta}=1$	0.3447 + 0.2799 = 0.6246	24.7134 + 24.7213 = 49.4347	0.9262 + 0.3770 = 1.3032	0.6147 + 0.4516 = 1.0663	299457.346

Table II. In *Step 6* we assume that the errors in voltage magnitude and SG active power are weighted by diagonal elements in matrix $\boldsymbol{W}$ in (13). Residuals and optimization criterion for results in Table II are shown in the tinted row in Table III. Sensitivity analysis with respect to the weighting factors ($\boldsymbol{W}$) is presented in Table III.

The reduced IEEE 14-bus test system is composed from:

- 36 state variables:
  - 22 for SGs (four 4-order (two of them are for SGe) and one 6-order models);
  - 12 for automatic voltage regulators (three 4-order models), and
  - 6 for turbines (two 3-order models).
- 35 algebraic variables:
  - 13×2 bus voltage magnitudes (V) and angles (θ);
  - 5×4 for SGs (P_m, P_g, Q_g, and v_f);
  - 3×1 for automatic voltage regulators (v_{fe});
  - 2×1 for turbines (v_{ft}).

The number of state (algebraic) variables is reduced from 53 (57) to 40 (51), or about 25% (11%). This reduction level is lower than in [20], and not very surprising given the strong couplings between areas.

Transient time responses (online measurements for original power system and after parameter estimation reduced power system) in equivalent SGes are shown in Fig. 4, where we compare the original transients for bus voltages and SGe's active powers (black solid line) with those produced by the reduced dynamic model (blue dashed line) after parameter estimation, where in Fig. 4a we show quantities for the actual SGs (retained area, buses 1 and 2), while in Fig. 4b we show transients for multiple SGes (reduced area, buses 10 and 14). For the retained part (Fig. 4a) we note an excellent agreement, while for reduced area (Fig. 4b) we note a satisfactory agreement. As expected, larger discrepancies are obtained for SGes (in buses 10 and 14). Larger errors in transients appear for active powers.

Step B: Improved re-optimized parameters.

Now we attempt to improve results shown in Fig. 4b; our hypothesis is that the SGe model is insufficient to capture dynamic REI of external area with coupled SG and DL dynamics. Thus, we use SGe+DLe in all boundary buses (2f, 5f, 10f and 14f in Fig. 3), where the initial parameters of the SGe take values from *Step A*. DLes in the external subsystem are assumed to be described by a 3-order dynamic model (see Appendix B for details). Constant (suggested in Step 4) and initial values of electrical parameters for the parameter esti-mation (in corresponding units) respectively are [23, Table II]:

- $r_s = 0.01$, $x_r = 0.15$, $x_\mu = 5.0$, $p_i = q_i = 0.333$.
- $x_s = 0.15$, $r_r = 0.05$, $p_p = 0.333$.

Obtained transient time responses are shown in Fig. 5 (for comparison purposes we display the same quantities as in Fig. 4b). From Fig. 5 we note much better agreement of time responses in non-reduced and reduced test systems.

In Table IV we show an analysis of oscillation modes (eigenvalues, frequencies and damping ratios) of the equilibrium point

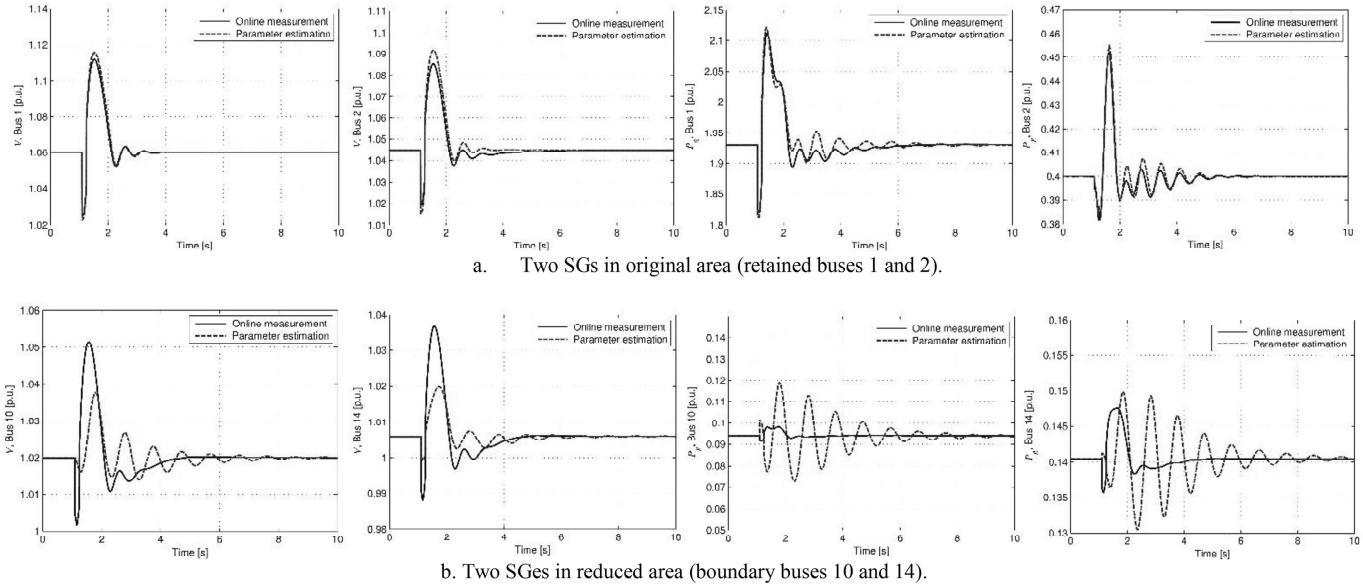

a. Two SGs in original area (retained buses 1 and 2).

b. Two SGes in reduced area (boundary buses 10 and 14).

Fig. 4. Transient responses (bus voltage magnitudes and SG active powers) of original and reduced IEEE 14-bus test systems (Step A: Initially optimized parameters).

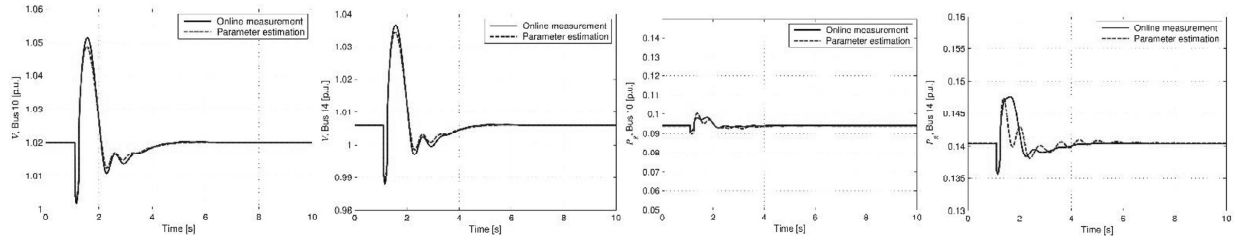

Fig. 5. Transient responses (bus voltage magnitudes and SG active powers) of original and reduced IEEE 14-bus test systems (Step B: Improved re-optimized parameters).

for non-reduced/reduced test systems. The following conclusions can be derived:

- Reduced test system has 36 eigenvalues (28 in retained dynamic elements and 8 in added dynamic elements (two 4-order equivalent SGs).
- Only two (non-critical) oscillation modes in retained dynamic elements have a frequency difference $>$0.1 Hz, compared with ones in the non-reduced test system (16th and 38, 39th).
- Only one (non-critical) oscillation mode in the retained dyna-mic elements has a damping ratio error $>$10%, compared with ones in the non-reduced test system (16th and 27, 28th).
- Oscillation modes in the added dynamic elements (two 4-order equivalent SGs) fully correspond to the missed oscillation modes, where the minimum damping ratios of the added oscillation modes are $>$7%.

Step C: Verification of parameters.

As every dynamic equivalent has to be robust for different operating conditions, we analyzed responses for different locations of the short circuit that initiates the transient, as shown in Fig. 6 (also see our results in Fig. 8). If necessary, additional re-optimization of parameters is possible, starting from values obtained in *Step B*.

B. Real-World Test System

The proposed model was tested on a realistic test system (Electric Power Industry of Serbia; a part of the ENTSO-E interconnection with 21177 buses, 30968 transmission lines and transformers, 1144 coupling devices (i.e., zero-impedance connections), 15756 loads, 4828 power plants, and 364 power system stabilizers) with: 441 buses, 655 branches (transmission lines and transformers), 72 SGs (43 of 4-order models and 29 of 6-order models), with automatic voltage regulators (AVRs) and turbine models, where AVRs and turbine are modeled by different numbers of equations. The dynamic model has total 850/1314 differential/algebraic variables. It is interconnected with neighboring countries over ten 400/220 kV lines, where eight lines (from buses 1, 2, 3, 4, 5, 7, 8, and 10) import energy, and two lines (from buses 6 and 9) export energy. External subsystems to be reduced are the national power systems with dominantly SG-based hydro/thermal production and mixed load consumption. Based on the conclusions derived in Section IV.A, all boundary buses are modeled by (SG+DL) dynamic equivalents (see Fig. 1).

We assume that the loop-flows among external power systems have a negligible influence on the retained power system. While convenient in allowing one-by-one reduction, the validity of this assumption is certainly system dependent.

TABLE IV
EIGENVALUES, FREQUENCIES, AND DAMPING RATIOS IN NON-REDUCED AND REDUCED POWER SYSTEMS (IEEE 14-BUS TEST SYSTEM) – SORTED BY THE REAL PART OF EIGENVALUES

Non-reduced test system				Reduced test system							
Oscillation modes				Oscillation modes in retained dynamic elements				Oscillation modes in added dynamic elements (two equivalent SGs)			
#	Eigenvalue	f [Hz]	ξ [%]	#	Eigenvalue	f [Hz]	ξ [%]	#	Eigenvalue	f [Hz]	ξ [%]
1,2	−1000.00±j0.00	159.15	100.00	1,2	−1000.00±j0.00	159.15	100.00				
3,4	−1000.00±j0.00	159.15	100.00								
5	−999.99	159.15	100.00								
6,7	−50.22±j284.65	46.00	17.38								
8,9	−50.10±j0.00	7.97	100.00	3	−50.29	8.00	100.00				
10,11	−49.95±j0.02	7.95	100.00	4	−49.95	7.95	100.00				
12	−49.94	7.95	100.00								
13	−27.56	4.39	100.00	5	−26.96	4.29	100.00				
14	−24.19	3.85	100.00								
15	−17.17	2.73	100.00								
16	−15.41	2.45	100.00	6	−14.20	2.26	100.00				
17	−10.29	1.64	100.00	7	−10.30	1.64	100.00				
18	−10.06	1.60	100.00	8	−10.07	1.60	100.00				
19	−6.64	1.06	100.00								
20	−6.35	1.01	100.00	9	−6.20	0.99	100.00				
21	−3.50	0.56	100.00	10	−3.39	0.54	100.00				
22,23	−2.91±j12.80	2.09	22.14	11,12	−3.39±j12.54	2.07	26.10				
24,25	−2.54±j9.73	1.60	25.24					13	−2.91	0.46	100.00
26	−2.14	0.34	100.00	16	−2.14	0.34	100.00				
27,28	−1.52±j11.16	1.79	13.48	14,15	−2.50±j10.21	1.67	23.80				
29,30	−1.25±j0.85	0.24	82.81								
31,32	−1.16±j1.28	0.27	67.05								
33,34	−1.14±j10.16	1.63	11.12	18,19	−1.15±j9.60	1.54	11.89				
35,36	−1.04±j1.12	0.24	68.03	20,21	−1.05±j0.86	0.22	77.26				
37	−1.02	0.16	100.00	22	−1.02	0.16	100.00	23,24	−1.01±j1.025	0.26	63.04
38,39	−1.02±j0.02	0.16	99.97	17	−1.81	0.29	100.00				
40,41	−1.01±j0.00	0.16	100.00	25	−0.98	0.16	100.00				
42,43	−1.00±j0.02	0.16	99.98	26	−0.95	0.15	100.00				
44,45	−0.74±j8.82	1.41	8.37					27,28	−0.65±j9.28	1.48	7.01
46,47	−0.64±j0.35	0.12	87.92	29	−0.65	0.10	100.00				
48,49	−0.59±j0.63	0.14	68.32	30	−0.54	0.09	100.00	31,32	−0.50±j7.11	1.13	7.03
50	−0.08	0.01	100.00	34	−0.08	0.01	100.00	33	−0.29	0.05	100.00
51	−0.02	0.00	100.00	35	−0.02	0.00	100.00				
52,53	−0.00±j0.00	0.00	100.00	36	−0.00	0.00	100.00				

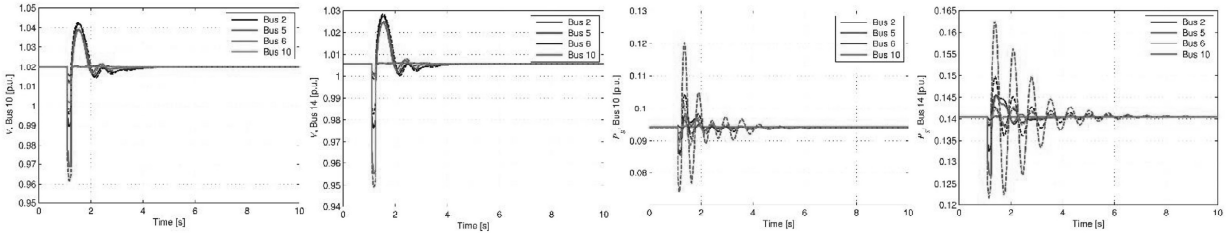

Fig. 6. Transient responses (bus voltage magnitudes and SG active powers) of original and reduced IEEE 14-bus test systems (Step C: Improved re-optimized parameters – note that online measurements in original test system are shown by solid lines, while by the dashed lines show the results obtained after parameter optimization of reduced test system).

Please note that the reduced test system (retained test system plus dynamic equivalents in boundary buses) represents about 2.2% of the whole ENTSO-E interconnection (for differential and algebraic parts).

The test system is subjected to the three-phase short circuit in bus 11 in $t = 0.05$ s, which cleared after 250 ms (fault impedance is $Z_f = \mathrm{j}\,0.1$ p.u.).

The computation time for a single transient analysis (for 10 s simulation time) for reduced test system is approximately 1.2 s.[3] The computational burden of time domain integration for the ENTSO-E transmission system are reported in [27;

[3]Intel(R) Core(TM) i7-6860HQ CPU @ 2.70 GHz, 64-bit Operating System, 32 GB RAM.

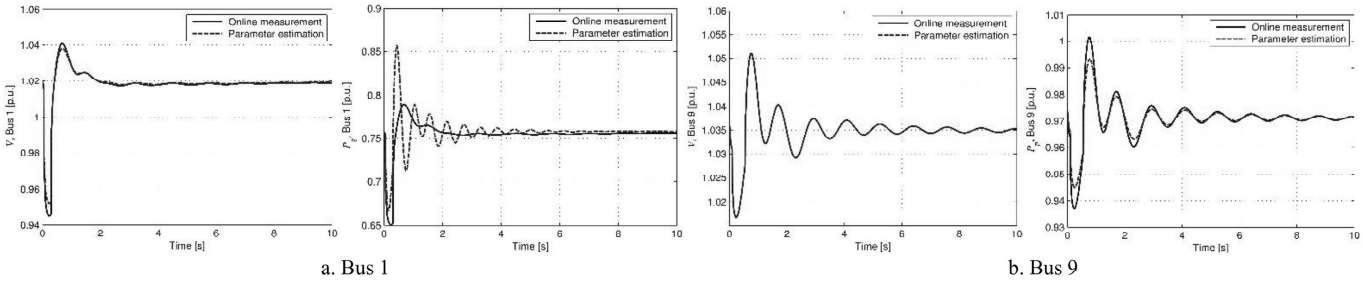

Fig. 7. Characteristic transient responses (bus voltage magnitudes and active powers) of original and reduced real-world test systems.

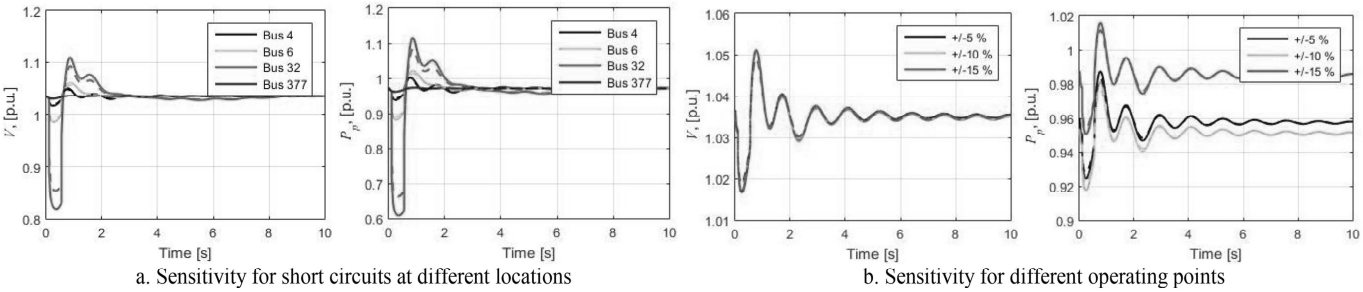

Fig. 8. Sensitivities of characteristic transient responses (bus voltage magnitudes and active powers) of original and reduced real-world test systems from Fig. 7 (case b. Bus 9) to short circuits at different locations and different operating points.

TABLE V
OPTIMAL PARAMETERS OF EQUIVALENT BRANCHES, SGES AND DLES (REAL-WORLD TEST SYSTEM)

Bus i	$\underline{Z}_{fi}+\underline{Z}_{gi}$ [p.u.]	$2H$ [MWs/MVA]	x_d [p.u.]	x'_d [p.u.]	x_q [p.u.]	x'_q [p.u.]	x_s [p.u.]	r_r [p.u.]	p_p
1	$(2.830+j8.490)\cdot10^{-5}$	8.350	1.306	0.246	1.306*	0.750	0.125	0.045	0.331
2	0.0178+j0.0534	7.432	2.320	0.926	1.905	1.651	0.131	0.037	0.402
3	$(3.560+j10.680)\cdot10^{-4}$	10.125	1.134	0.870	0.980	0.692	0.182	0.044	0.365
4	$(2.125+j6.375)\cdot10^{-4}$	9.320	1.116	0.138*	0.985	0.138	0.172	0.048	0.295
5	$(0.830+j2.490)\cdot10^{-3}$	5.650	1.971	0.975	1.562	1.103	0.152	0.041	0.310
6	0.0130+j0.0390	7.130	1.834	0.892	1.324	1.123	0.145	0.038	0.382
7	$(2.125+j6.375)\cdot10^{-4}$	8.215	2.145	1.113	1.234	2.145*	0.134	0.035	0.412
8	$(0.934+j2.802)\cdot10^{-3}$	9.267	2.116	1.001	1.752	1.120	0.161	0.046	0.456
9	0.0010+j0.0030	11.560	1.913	0.852	1.224	1.015	0.123	0.046	0.512
10	$(8.540+j25.620)\cdot10^{-4}$	12.050	1.326	0.323	2.101	0.635	0.185	0.052	0.342

*Active constraints $x_d \geq x_q > x'_q \geq x'_d \geq 0$.

Table V] for different methods (software and hardware specifications are provided in p. 8, second column). These values vary from 20 to 40 s (for 5 s simulation time). These values are relevant for orientation only – our Matlab code is not optimized for speed and thus not readily comparable with Python code in [27]. Regardless, the expected reduction in the computation time is clear, and, in our experience, it exceeds proportionally the reduction in the number of differential and algebraic equations.

However, reduction in computational effort is not the main motivation for dynamic equivalents today. The main reason is the uncertainty in such large models, with parametric uncertainty being one of the key aspects. The main reasons for the lack of model fidelity are reviewed in the Introduction.

Optimal parameter identification for equivalent branches, SGes and DLes are presented in Table V.

Transient time responses (online measurements for the retained test system and with optimal parameter estimation for reduced test system) in fictitious buses are shown in Fig. 7.

Sensitivities of characteristic transient responses (bus voltage magnitudes and active powers) of the original and reduced real-world test systems from Fig. 7 (case b. Bus 9) to short circuits at different locations and different operating points (obtained by the random variation of active/reactive loads and active power generations) are shown in Fig. 8.

V. CONCLUSION

In this paper we describe a modified Radial, Equivalent and Independent (REI) procedure for estimating a dynamic equivalent of a power system area from available online measurements

at boundary buses. The procedure is illustrated on Synchronous Generator (SG) based equivalent and Dynamic Load (DL) based equivalent in two multi-machine benchmark power systems. It is also applicable to identification of other dynamical components (e.g., inverter-connected sources). Advantages of the proposed method include minimal assumed knowledge about the area to be reduced, and very promising scaling properties (depending only on measurements). Potential downsides include neglected dynamics of automatic voltage regulators and turbines (for SG parameter identification). We feel that this will be useful for future interconnections which will be more variable (due to say renewable sources and dynamically aggregated loads such as microgrids), while market forces may hinder the motivation to share sensitive technical data with competitors.

APPENDIX A
SG-BASED EQUIVALENT (SGE)

For SGe the common mechanical differential equations (2-order model) can be written as [26, eq. (15.5)]:

$$\boldsymbol{f} \Rightarrow \begin{cases} \dot{\delta} = \Omega_b(\omega - \omega_s) \\ \dot{\omega} = \dfrac{1}{2H}\left(\tau_m - \tau_e - D(\omega - \omega_s)\right) \end{cases} \tag{A1a}$$

where for $\omega \approx \omega_s$, ($\omega \approx 1\ p.u.$ and assumed $r_a \approx 0$ for simplicity):

$$\begin{aligned} \tau_e &= P_g/\omega \approx P_g = v_d i_d + v_q i_q \\ Q_g &= v_q i_d - v_d i_q. \end{aligned}$$

For one q-axis and one d-axis, 4-order model to (A1a) the following differential equations are added [26, eq. (15.19)]:

$$\boldsymbol{f} \Rightarrow \begin{cases} \dot{e}'_q = \dfrac{1}{T'_{d0}}\left(-e'_q - (x_d - x'_d)i_d + v_f\right) \\ \dot{e}'_d = \dfrac{1}{T'_{q0}}\left(-e'_d - (x_q - x'_q)i_q\right) \end{cases} \tag{A1b}$$

where $v_d - e'_d = x_q i_q$ and $e'_q - v_q = x'_d i_d$.

The common algebraic equations are:

$$\boldsymbol{g} \Rightarrow \begin{cases} 0 = \tau_{m0} - \tau_m \\ 0 = v_{f0} - v_f \\ v_d = V\sin(\delta - \theta) \\ v_q = V\cos(\delta - \theta) \end{cases} \tag{A2}$$

APPENDIX B
DYNAMIC LOAD BASED EQUIVALENT (DLE)

Static Voltage Dependent equivalent (SVDe) part

The static voltage dependent, or ZIP, load part can be described as [26, eq. (14.3)]:

$$P_{SVD} = p_z\left(\frac{V}{V_0}\right)^2 + p_i\left(\frac{V}{V_0}\right) + p_p \tag{A3}$$

$$Q_{SVD} = q_z\left(\frac{V}{V_0}\right)^2 + q_i\left(\frac{V}{V_0}\right) + q_p \tag{A4}$$

Induction Machine based equivalent (IMe) part

The differential equations for IM-based equivalent part are:

$$\boldsymbol{f} \Rightarrow \begin{cases} \dot{\sigma} = \dfrac{1}{2H_m}(\tau_m - \tau_e) \\ \dot{e}'_d = \Omega_b \sigma e'_q - \dfrac{1}{T'_0}\left(e'_d + (x_0 - x')i_q\right) \\ \dot{e}'_q = -\Omega_b \sigma e'_d - \dfrac{1}{T'_0}\left(e'_q - (x_0 - x')i_d\right) \end{cases} \tag{A5}$$

where:

$\tau_m = \alpha + \beta\sigma + \gamma\sigma^2$ (α, β and γ are the coefficients for the mechanical torque, where $\alpha + \beta + \gamma = 1$);

$$\begin{aligned} \tau_e &= P_{IM}/\omega \approx P_{IM} = v_d i_d + v_q i_q; \\ Q_{IM} &= v_q i_d - v_d i_q; \\ x_0 &= x_s + x_\mu; \\ x' &= x_s + \frac{x_r x_\mu}{x_r + x_\mu}; \\ T'_0 &= \frac{x_r + x_\mu}{\Omega_b x_\mu}; \\ v_d - e'_d &= r_s i_d - x' i_q; \\ v_q - e'_q &= r_s i_q + x' i_d. \end{aligned}$$

The common algebraic equations are:

$$\boldsymbol{g} \Rightarrow \begin{cases} v_d = -V\sin\theta \\ v_q = V\cos\theta \end{cases} \tag{A6}$$

REFERENCES

[1] G. Andersson *et al.*, "Causes of the 2003 major grid blackouts in North America and Europe, and recommended means to improve system dynamic performance," *IEEE Trans. Power Syst.*, vol. 20, no. 4, pp. 1922–1928, Nov. 2005.

[2] F. Milano and K. Srivastava, "Dynamic REI equivalents for short circuit and transient stability analyses," *Electr. Power Syst. Res.*, vol. 79, no. 6, pp. 878–887, Jun. 2009.

[3] A. T. Sarić and A. M. Stanković, "Integration of equation and signal-based models in transient analysis of electric energy systems," *IEEE Trans. Circuits Syst. I*, vol. 53, no. 7, pp. 1589–1596, Jul. 2006.

[4] IEEE Task Force on Dynamic System Equivalents, "Dynamic system equivalents: A survey of available techniques," *IEEE Trans. Power Del.*, vol. 27, no. 1, pp. 411–420, Jan. 2012.

[5] X. Lei, D. Povh, and O. Ruhle, "Industrial approaches for dynamic equivalents of large power systems," in *Proc. IEEE Power Eng. Soc. Winter Meeting*, Jan. 2002, pp. 1036–1042.

[6] P. Ju, L. Q. Ni, and F. Wu, "Dynamic equivalents of power systems with online measurements. Part 1: Theory," *IEE Proc., Gener. Transm. Distrib.*, vol. 151, no. 2, pp. 175–178, Mar. 2004.

[7] F. Ma and V. Vittal, "Right-sized power system dynamic equivalents for power system operation," *IEEE Trans. Power Syst.*, vol. 26, no. 4, pp. 1998–2005, Nov. 2011.

[8] J. H. Chow, Ed., *Power System Coherency and Model Reduction*. New York, NY, USA: Springer, 2013.

[9] U. D. Annakkage *et al.*, "Dynamic system equivalents: A survey of available techniques," *IEEE Trans. Power Del.*, vol. 27, no. 1, pp. 411–420, Jan. 2012.

[10] J. J. Sanchez-Gasca *et al.*, "Trajectory sensitivity based identification of synchronous generator and excitation system parameters," *IEEE Trans. Power Syst.*, vol. 3, no. 4, pp. 1814–1822, Nov. 1988.

[11] S. M. Benchluch and J. H. Chow, "A trajectory sensitivity method for the identification of nonlinear excitation system models," *IEEE Trans. Energy Convers.*, vol. 8, no. 2, pp. 159–164, Jun. 1993.

[12] I. A. Hiskens, "Nonlinear dynamic model evaluation from disturbance measurement," *IEEE Trans. Power Syst.*, vol. 16, no. 4, pp. 702–710, Nov. 2001.
[13] M. Burth, G. C. Verghese, and M. Velez-Reyes, "Subset selection for improved parameter estimation in on-line identification of a synchronous generator," *IEEE Trans. Power Syst.*, vol. 14, no. 1, pp. 218–225, Feb. 1999.
[14] E. Cari and L. F. C. Alberto, "Parameter estimation of synchronous generators from different types of disturbances," in *Proc. IEEE Power Energy Soc. Gen. Meeting*, Jul. 2011, pp. 1–7.
[15] P. Ju, L. Q. Ni, and F. Wu, "Dynamic equivalents of power systems with online measurements. Part 1: Theory," *IEE Proc., Gener., Transm., Distrib.*, vol. 151, no. 2, pp. 175–178, Mar. 2004.
[16] P. Ju, F. Li, N. G. Yang, X. M. Wu, and N. Q. He, "Dynamic equivalents of power systems with online measurements Part 2: Applications," *IEE Proc., Gener., Transm., Distrib.*, vol. 151, no. 2, pp. 179–182, Mar. 2004.
[17] Z. Huang *et al.*, "Generator dynamic model validation and parameter calibration using phasor measurements at the point of connection," *IEEE Trans. Power Syst.*, vol. 28, no. 2, pp. 1939–1949, May 2013.
[18] M. Shiroei, B. Mohammadi-Ivatloo, and M. Parniani, "Low-order dynamic equivalent estimation of power systems using data of phasor measurement units," *Int. J. Electr. Power Energy Syst.*, vol. 74, pp. 134–141, Jan. 2016.
[19] M. Gavrilas, O. Ivanov, and G. Gavrilas, "REI equivalent design for electric power systems with genetic algorithms," *WSEAS Trans. Circuits Syst.*, vol. 7, no. 10, pp. 911–921, Oct. 2008.
[20] A. T. Sarić, M. K. Transtrum, and A. M. Stanković, "Dynamic model estimation for power system areas from boundary measurements," in *Proc. IEEE Power Energy Soc. Gen. Meeting*, Jul. 2016, pp. 1–5.
[21] M. K. Transtrum and J. P. Sethna, "Improvements to the Levenberg-Marquardt algorithm for nonlinear least-squares minimization," unpublished paper, 2012. [Online]. Available: http://www.arxiv.org/abs/1201.5885
[22] M. K. Transtrum, A. T. Sarić, and A. M. Stanković, "Measurement-directed reduction of dynamic models in power systems," *IEEE Trans. Power Syst.*, vol. 32, no. 3, pp. 2243–2253, May 2017.
[23] C. F. Youn, A. T. Sarić, M. K. Transtrum, and A. M. Stanković, "Information geometry for model reduction of dynamic loads in power systems," in *Proc. IEEE PowerTech Conf.*, Manchester, U.K., Jun. 2017, pp. 1–6.
[24] P. Kundur, *Power System Stability and Control*. New York, NY, USA: McGraw-Hill, 1994.
[25] M. R. A. Paternina, J. M. Ramirez-Arredondo, J. D. Lara-Jiménez, and A. Zamora-Mendez, "Dynamic equivalents by modal decomposition of tie-line active power flows," *IEEE Trans. Power Syst.*, vol. 32, no. 2, pp. 1304–1314, Mar. 2017.
[26] F. Milano, *Power System Modeling and Scripting*. New York, NY, USA: Springer, 2010.
[27] F. Milano, "Semi-implicit formulation of differential-algebraic equations for transient stability analysis," *IEEE Trans. Power Syst.*, vol. 31, no. 6, pp. 4534–4543, Nov. 2016.

Andrija T. Sarić was born in 1962. He received the B.Sc., M.Sc., and Ph.D. degrees in electrical engineering from the University of Belgrade, Belgrade, Serbia, in 1988, 1992, and 1997, respectively. He is currently a Full Professor in electrical engineering with the Faculty of Technical Sciences, University of Novi Sad, Serbia. His main research interests include power system analysis, optimization, and planning, as well as the application of artificial intelligence methods in these areas.

Mark K. Transtrum received the Ph.D. degree in physics from Cornell University, Ithaca, NY, USA, in 2011. He then studied computational biology as a Postdoctoral Fellow from MD Anderson Cancer Center, Houston, TX, USA. He has been an Assistant Professor in physics and astronomy with Brigham Young University, Provo, UT, USA, since 2013. His work considers representations of a variety of complex systems including power systems, systems biology, materials science, and neuroscience.

Aleksandar M. Stankovic (F'05) received the Ph.D. degree in electrical engineering from the Massachusetts Institute of Technology, Cambridge, MA, USA, in 1993. He is currently an A.H. Howell Professor with Tufts University, Medford, MA, USA. He was with Northeastern University, Boston, MA, USA, from 1993 to 2010. He has held visiting positions with the United Technologies Research Center, and at L'Universite de Paris-Sud and Supelec. He is a Co-Editor of book series on power electronics and power systems for Springer. He has served as an Associate Editor for the IEEE TRANSACTIONS ON POWER SYSTEMS, IEEE TRANSACTIONS ON SMART GRID, and IEEE TRANSACTIONS ON CONTROL SYSTEM TECHNOLOGY.